Contents lists available at Science-Gate

International Journal of Advanced and Applied Sciences

Journal homepage: http://www.science-gate.com/IJAAS.html

Hybrid optimization in loop: 3D human body reconstruction from basic information

Tran Van Duc [1], Nguyen Tien Dat [1,*], V. L. Nguyen [2]

[1]Modeling and Simulation, Viettel High Technology Industries Corporation, Hanoi, Vietnam
[2]Institute of Engineering and Technology, Thu Dau Mot University, Binh Duong Province, Vietnam

ARTICLE INFO

Article history:
Received 28 September 2021
Received in revised form
24 December 2021
Accepted 24 December 2021

Keywords:
Human shape reconstruction
Parametric model
Hybrid optimization
Weight correction

ABSTRACT

3D human reconstruction is widely used for digital transformation in different industries such as e-retail, entertainment, health care, epidemiology. For practical applicability, the modeling process is required to be quick, affordable while still ensuring capabilities in reconstruction accuracy and reliability. To meet such business requirements, we propose a novel technique for producing an exact 3D human body using only basic anthropomorphic measurements. To begin, the paper refers to and summarizes core technologies of the three most common 3D human reconstruction approaches, including (1) Using Point Clouds, (2) Using Images, and (3) Using Anthropometric Measurements. Despite successfully recreating 3D human shapes, these methods face problems of long processing time and high investment cost, making the solution impractical for mass use. Moreover, in the human reconstruction sector particularly, the variety of human shapes, poses, and clothing poses a significant challenge to output accuracy. In this regard, our method combines (1) a local optimization model for determining hyperparameters for classifying different human shapes and (2) a global optimization for reconstructing 3D models, allowing reconstruction of both naked human bodies and clothed ones. The proposed method was evaluated quantitatively and qualitatively using a real dataset to demonstrate its feasibility and efficiency when used in real-world applications.

1. Introduction

In recent years, 3D human reconstruction has been extensively used in different industries. For example, in the medical field, the 3D reconstruction technique allows doctors and technologies to capture the image of patients in a 3D format and obtain information about their outer body parts in a few seconds. This information has implications for a variety of states of health, for example, based on the body size and shape, doctors can diagnose and manage obesity treatment. As for the fashion industry, due to the Covid-19 pandemic, numerous fashion and apparel companies are leveraging online channels to boost their sales. In this application, 3D human reconstructing technology creates shopper's 3D avatars and enables them to try garments on their "twin" without going to physical stores, helping sellers to enhance customer experience and competitiveness on the market. Other fields such as Entertainment, Ergonomics, Anthropometry also leverage this technology to better serve their purpose. Due to this wide application and huge demand, 3D human reconstruction has attracted great research interest. Generally, there are two main approaches to digitalize the 3D human model: (1) Using a parametric model, (2) Using traditional scanners. The first method produces an acceptable accuracy in both generated shape and pose and its processing time is also appropriate. However, it requires a large dataset to generate the parametric model, which is considered a weakness of this method. For the second approach, the precise and high-resolution results are the main strong point. Nevertheless, this method requires high equipment costs while processing time is rather slow, preventing scanners from being widely adopted around the world.

This research proposes a new technique to estimate the 3D body human from 2D images and basic information such as height, weight, age, and

* Corresponding Author.
Email Address: datnt65@viettel.com.vn (N. T. Dat)
https://doi.org/10.21833/ijaas.2022.02.016
Corresponding author's ORCID profile:
https://orcid.org/0000-0002-7537-8708

gender of the digitized person. A parametric model (SMPL) by Loper et al. (2015) is used with several customizations to adjust and create the 3D model by pose and shape parameters. This method has had several approaches, some of them focus on the accuracy of the human pose when creating 3D models, others put the main force in the shape while there are a few researchers developing different points of view with estimating body under clothing. In general, most methods face three main challenges: (1) The total time to reconstruct body shape, (2) the accuracy for reconstructing the human body with clothes, (3) the ease to be compatible and integrated on multiple platforms.

The main contributions of this research are summarized below: (1) A double loop optimization is used for classifying human types and estimating the 3D shape under clothing, (2) Thanks to applying weight and age of the digitized person in the whole process, segmentation module is eliminated. This results in reduced processing time and dependence on the segmentation stage. (3) A parametric model with normalized shape is applied to replace the calibration process, allowing wide application in popular devices. The research is organized as follows: Section II summarizes previous works on estimating 3D body human. The proposed method is detailed in Section III, followed by research results and discussion in Section IV. Section V concludes the paper.

2. Related works

Recent researches have a significant improvement in reconstructing 3D human model based on multiple approaches. In this part, three main methods including: (1) Using 2D Images, (2) Using Anthropometric measurements, (3) Using Point Cloud are introduced and analyzed in terms of their upsides and downsides.

2.1. 3D reconstruction from images

Bogo et al. (2016) used an RGB image to estimate the 3D pose and shape of the human body. A Convolutional Neural Network (Deep-cut) is used to predict 2D joint locations, then an objective function that penalizes the error between detected 2D joint locations and projected 3D model joints is applied to fit the statistical body shape model. Kanazawa et al. (2018) proposed a real-time framework for recovering the 3D joint locations and shape of the body from a single RGB image. The key point is to pass an image through a convolutional encoder to collect the main features and send them to the iterative 3D regression module. This module aims to infer the 3D human body and the camera so that valuable information in context and two training stages would not be missed. The advantages of this framework are the run time and 3D joint errors. However, regarding estimating human body shape, this approach could not produce an acceptable result. Different from the above approaches, Shigeki et al., (2018) combined the optimization-based method with a regression-based method to form a new one called SPIN (SMPL optimization IN the loop). The objective is to initialize an iterative optimization from a regressed estimate of the network that speeds up the fitting process and leads the optimization to more accurate model fits compared to SMPLify (Bogo et al., 2016) or HMR (Kanazawa et al., 2018). SPIN is divided into two main parts: (1) applying the Convolution Neural Network to predict the regressed shape parameters, (2) using the same routine as SMPLify (Bogo et al., 2016) to optimize the 3D Shape. Results on the Human 3.6M dataset and MPI-INF-3DHP proved the efficiency of this method as state-of-the-art in pose estimation. However, once again, it is not suitable for shape estimation. Zeng et al. (2017) defined a CNN that reconstructed the 3D human body from two orthogonal silhouettes images. The authors investigated a neural network to estimate shape parameters of a parametric model called: SMPL. The dataset for the training network is a combination of real- and augmented-dataset which is generated from SMPL by using K-nearest neighbor. Testing results indicated the effectiveness of this method in modeling 3D human bodies from two silhouette images. However, this approach requires users to wear skin-tight clothes or be naked to derive his/her body shape model. Additionally, incorrect orthogonal views could adversely affect the final result. Song et al. (2018) proposed an approach to estimate 3D pose and shape under clothing from a single RGB image. The key point is to use a clothing region segmentation in addition to cloth-skin displacement modeling. The optimization has the same concept as SMPLify, however, two terms: (1) skin contours and (2) clothed contours are added into the objective function to find the optimal solution for shape and pose parameters in the parametric model. The experiment indicated a more accurate result in body shape modeling compared to others. However, the displacement between clothed and naked contour is dependent on auto-encoder-based image generation.

2.2. 3D reconstruction from anthropometric measurements

Wuhrer and Shu (2013) presented a feature-selection-based local mapping method using anthropometric measurements. It consists of three modules: (1) Selector, (2) Imputer, (3) Mapper. The Selector is created by using a dataset of 3D body meshes and anthropometric measurements as input. Its outputs are relevance masks and mapping matrices that would be used in the Mapper module. Imputer indicates missing data from user's input and passes them to the Mapper, combining with masks and matrices above to generate 3D body meshes. Pujades et al. (2019) used a mesh-based deformation to optimize the sought measurements. It is divided into two main steps: (1) finding an initial solution based on the learned correlation that closes to the real solution, (2) using two steps of non-linear optimization to reshape the body in both local shape and other shape variations that are not presented in the training database. Fig. 1 shows an overview of the proposed method.

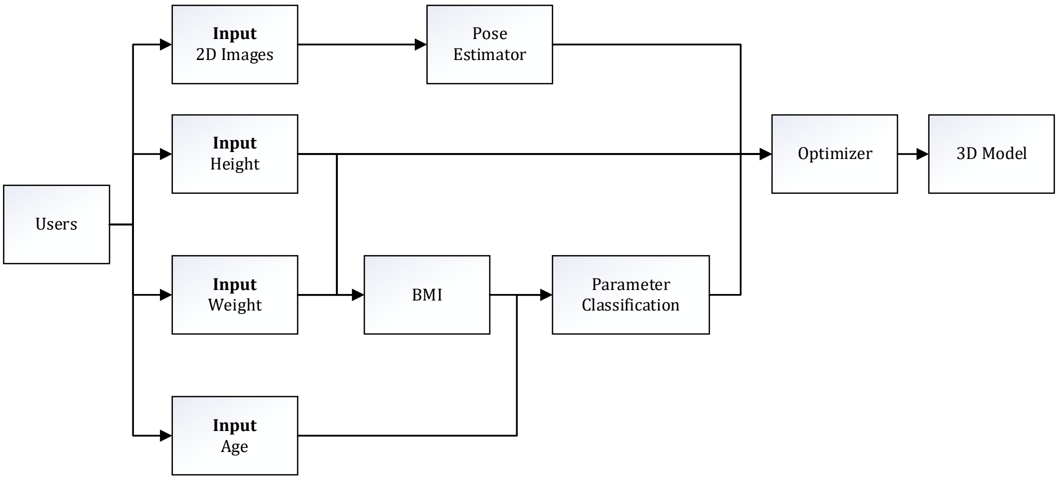

Fig. 1: An overview of the proposed method

Nguyen and Hoang (2021) proposed a rapid method to reconstruct an avatar from 3D measurements. The key factor is to use the linear relation between the measurements and the body shape space via linear regressors. It leads to a real-time tool with acceptable results from using fewer measurements. Zhang and Chen (2001) used the heuristic optimization method to find the shape parameters from measurements. This approach yields a good result of body shape in an acceptable processing time. However, the weakness of all methods above is the requirement of input parameters. In particular, incorrect input parameters could cause inaccurate results when creating a 3D model of users.

2.3. 3D reconstruction from point cloud

Liu et al. (2019) proposed a method that uses two depth images of front-facing and back-facing bodies to create the 3D human model. It consists of three phases: (1) Pose Estimation: A template mesh is selected and pose parameters of the parametric model are estimated based on two input point clouds; (2) Shape Reconstruction: the input point clouds register the template and create in PCA shape spaces; (3) Front- registered and back registered are stitched and refined in a 3D body shape. Results on the PDT13 dataset and Hasler's dataset proved the efficiency of this method with a mean error of vertex to vertex approximately 8.0 mm. However, similar to the two approaches above, it could not estimate the body shape under clothing and requires specific hardware devices to be implemented.

3. Methodology

Fig. 1 indicates an overview of our proposed method. A parametric model called: A Skinned Multi-Person Linear (SMPL) is used to reshape the body model. It is defined as a function of three parameters: Shape β, Pose θ, Translation Ψ and the output is a triangle surface with 6890 vertices. However, to not calibrate input images, a variant of SMPL is presented and described in detail below.

The system's input parameters include height, weight, age, and 2D front-view images of the digitized person. We focus on finding the optimal solution for shape and pose parameters applying Adam optimization to minimize the objective function. There are three error terms: Joint-based data term E_J^m, shape prior term E_β^m and a weight correction term E_{weight}^m as following:

$$E^m = \omega_J . E_J^m(\theta^m, \beta^m, K^m, J_e^m) + \omega_{weight} . E_{weight}^m + \omega_\beta . E_\beta^m \tag{1}$$

where ω_J, ω_{weight}, ω_β are scalar weights; θ^m, β^m are pose and shape parameters; K^m is camera parameter; J_e^m are 2D joints estimated from MediaPipe for a specific sample m, which is a machine learning solution for high fidelity body pose tracking of Google. The predicted output of 33 pose landmarks is used to estimate pose parameters θ. E_J^m, E_β^m are built similarly in the SMPLify (Bogo et al., 2016).

3.1. Weight correction term

The term regarding weight is added to the objective function. The formula 2 below shows the detail of this term where: pd_weight is the estimated weight, gt_weight is the expected value of users, ε^n is the correction weight that is generated based on the dataset information with Body Mass Index (BMI) and age using optimization in the loop.

$$E_{weight} = \| pd\_weight^m - gt\_weight^m + \varepsilon^n \| \tag{2}$$

Fig. 2 shows the linear relationship between weight and volume.

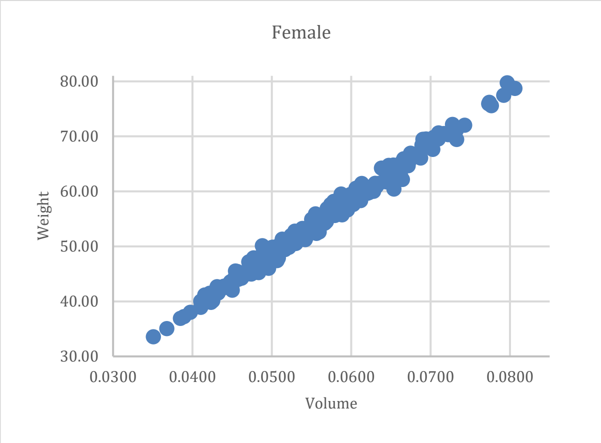

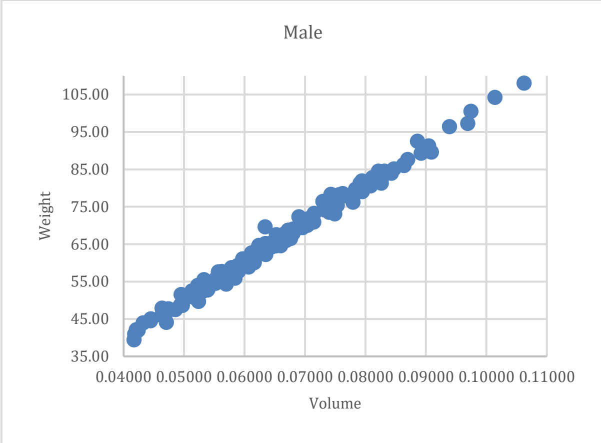

Fig. 2: The linear relationship between weight and volume

There are two key points: (1) Estimating the weight of the approximate model after each iteration, (2) Identifying the correction weight based on the BMI and age. Due to the complexity of directly calculating weight, we define a method to estimate the weight via two steps: (1) Converting the triangle mesh to volume as ref (WHO, 2000), (2) Using a linear regressor to estimate weight by respective volume. The concept of calculating the volume of mesh is to estimate the volume of each mesh and make an accumulation. For each triangle of the model, its vertices are connected with the origin and form a tetrahedron and the volume of the tetrahedron is as follows: $V = \frac{1}{6}(v_1 \times v_2).v_3$.

To deal with weight scalar, a classification of weight by BMI in Asian adults is followed as ref (Pishchulin et al., 2017). Based on the characteristic of ages in the dataset, two main groups are divided: Lower than 44 years old and is equivalent and higher than 44 years old. The detail is presented in Table 1.

Table 1: Classification of correction weight parameters based on BMIs and ages

Age / BMI	< 44	≥ 44
Underweight	ε^1	ε^6
Average	ε^2	ε^7
Overweight at risk	ε^3	ε^8
Overweight Obese 1	ε^4	ε^9
Overweight Obese 2	ε^5	ε^{10}

$\varepsilon^n \in \{\varepsilon^1, \varepsilon^2, \varepsilon^3, \varepsilon^4, \varepsilon^5, \varepsilon^6, \varepsilon^7, \varepsilon^8, \varepsilon^9, \varepsilon^{10}\}$

The next step is to find the weight scalar as defined above. This would be generated at the offline stage by minimizing the formula:

$$E_{mea} = \sum_m \sum_n \|pd\_\mathcal{M}_n^m - gt\_\mathcal{M}_n^m\| \quad (3)$$

where $pd\_\mathcal{M}_n^m$, $gt\_\mathcal{M}_n^m$ are respectively predicted measurement and ground truth measurement of sample m and anthropometric measurement n. To account for the relationship between volume and weight, a linear regressor is created by using a real dataset on Vietnamese collected by Viettel Military Industry and Telecoms Group (Viettel dataset). Fig. 2 indicates the linear relationship between weight and volume, and the formula is: $y = X\beta + \varepsilon$, where X is the volume, y is the weight, β and ε are scalars.

3.2. Normalized height parametric model

As mentioned above, a new technique is defined to solve the issue with unknown intrinsic and extrinsic parameters. A normalized height model is created by using Principal Component Analysis (PCA) for the dataset (Zhang and Chen, 2001) with 3000 samples both in males and females. All samples under point cloud format are aligned and fitted to a topology mesh to ensure the similarity in height and pose using a non-rigid registration strategy in Fan et al. (2004). The number of dimensionalities in the shaping model is defined to ensure the maximum variance of approximately 95.45%.

3.3. Optimization

First, to estimate correction weight ε^n, we conduct an optimization process: applying an outer loop for the whole dataset of human body shape collected according to Table 1 and an inner loop for each individual in the dataset.

For the outer loop optimization, the normalized height model is utilized to register all samples in this dataset and extract the ground truth measurement of the registered model. The correction weight ε^n is initialized at one matrix and the inner optimization loop is applied to predict measurements of each individual in the dataset. The value of ε^n is changed constantly to minimize the objective function E_{mea}. In that case, only three measurements are used to estimate weight scalar: Chest circumference, waist circumference, and hip circumference. For this selection, two factors are ensured: Convergence of optimization algorithms and sufficient information with three main anthropometric measurements.

For the inner loop optimization, the main routine is divided into two main steps. In the first step, camera translation and body orientation are optimized by minimizing the objective function E_m^J over the shoulder and hip joints. After the camera translation and body orientation are defined, the second step performs estimating the θ^m, β^m, K^m parameters at the same time by minimizing the objective function E_m over the whole joint as predicted above. To improve the performance of the optimization process, first ω_{weight} was initialized at a small value and then increased in each iteration. Fig. 3 shows a brief description of measurements.

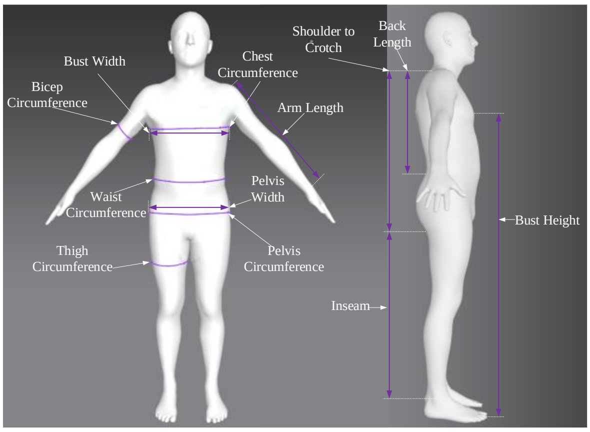

Fig. 3: A brief description of measurements

3.4. Measurements

The anthropometric measurements are divided into two main groups: Euclidean that is calculated from the distance between two vertices and Circumference computed from the intersection of the model to the plane using an algorithm called convex hull to estimate the polygonal chains. Due to the constant in the topology of a model after reconstructing, an intersecting plane is defined by a vertex at the expected measurement position and its normal direction. The way to measure is specified for main circumferences like chest, waist, and hip.

4. Result and discussion

This section indicates the quantitative and qualitative results which were verified on the Viettel dataset. This dataset includes more than 900 samples with different gender, occupation, region, pose and body mass index to ensure the diversity of the population in Vietnam. The process is deployed and run on Quadro P4000 (NVIDIA GeForce/8GB/DDR5/256 Bit). This dataset is divided into two parts with the ratio of 70%-30%: The formal is used for estimating correction weight parameters which are described above and the latter is applied for validating and verifying the proposed algorithm. The results would be run on other methods: SPIN and Silhouettes-based-HSE (SBHSE).

4.1. Quantitative results

We test quantitative results with two datasets: (1) First dataset without clothes, people are required to wear only bra and swimwear and (2) Second dataset with clothes, there is no requirement for models' outfit, meaning that they can wear any garments (shirt, Tshirt, dress, pants, shorts, coat, etc.) in any styles (slim-fit, regular-fit, oversized) and mixing with different accessories such as watch, necklace, ring, bag, and shoes. Due to a large number of results, the detail would be put in Appendix A. Only major figures are used and analyzed in this part to evaluate the effectiveness of the proposed method. Fig. 4 illustrates the comparison results between three methods in females and males without clothes. The information shows the average errors of 13 anthropometric measurements in millimeters. Overall, SPIN has the worst accuracy in shape reconstruction. Ours and SBHSE have similarities with a mean error approximately lower than 20mm. Besides, the results in SPIN are not stable. It gives better accuracy in chest, waist circumferences with females but worse in other measurements, greater than 60mm. However, with the measurements which are defined by Euclidean distance such as back length, chest width, pelvis width, the errors are improved, approximately lower than 40mm. Back to ours and SBHSE, the errors are maintained in the range of [1mm–20mm]. Furthermore, there is no big difference between circumference and linear measurements.

Fig. 5 indicates the mean errors of humans with clothing. Overall, SPIN and SBHSE do not give feasible results in shape reconstruction. The average errors are 57.45mm, 48.96mm with females, and 47.60mm, 48.96mm with males, respectively. Meanwhile, it is approximately 10.72mm and 9.58mm in our method. It is easy to be seen that the main errors come from circumferences where the information of users is missing out due to wearing clothes. These errors with SBHSE are about 100mm for chest, waist, and pelvis, both in females and males. However, the linear measurements are better and still remain the accuracy as running without clothing. On the other hand, ours brings a huge difference in almost all of the measurements, both in circumference and linear measurements. Besides, the average processing time of SPIN, SBHSE, and ours are 0.2s, 5.5s, and 10.2s respectively. Compared to Scanning systems such as TC^2, Vitronics, Wicks and Wilson TriForm (Fan et al., 2004) whose total capturing and processing time for reconstructing the human body are 53s, 40s, and 252s respectively, our proposed technique could yield better accurate results than other parametric approaches and be quicker than traditional scanners simultaneously.

4.2. Qualitative results

Fig. 6 proves the efficiency of our method in estimating and applying real data. The model and algorithm are contained as API and deployed on Amazon TC2 with g4dn.xlarge and then implemented on a mobile application to test the result. People with different BMI wearing casual clothes are recruited to this experiment. It can be seen on the results in SPIN and SBHSE, the shapes of body human in both front view and side view are not accurate compared to ground truth, especially in shape generated by SPIN. Looking into three measurements shown in Fig. 6, an imprecision in outputs of SPIN and SBHSE could be seen clearly. The mean errors are respectively 1.59, 15.2, 8.4cm in our approach, SPIN, and SBHSE. The accuracy of our method is better with chest and pelvis circumference, the errors are smaller than 1cm, slightly increase in the waist but remain smaller than 2.5cm.

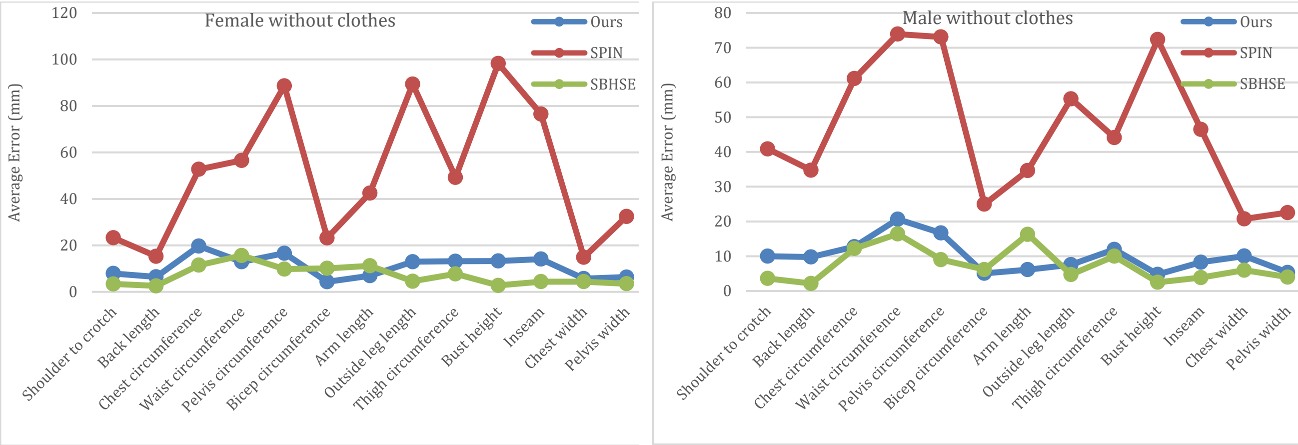

Fig. 4: Quantitative results of females and males without clothes

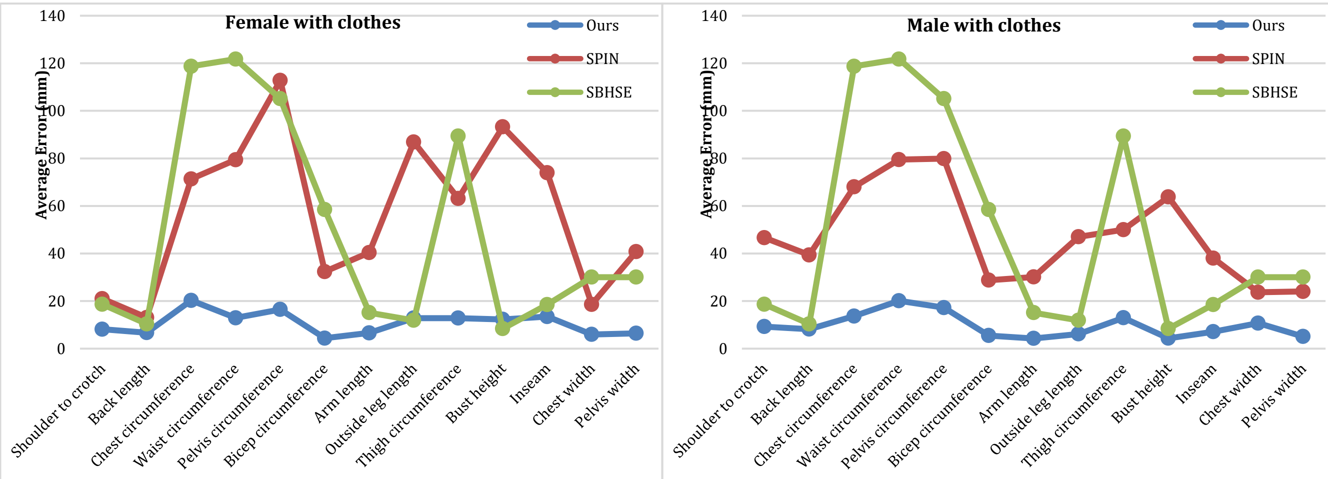

Fig. 5: Quantitative results of females and males with clothes

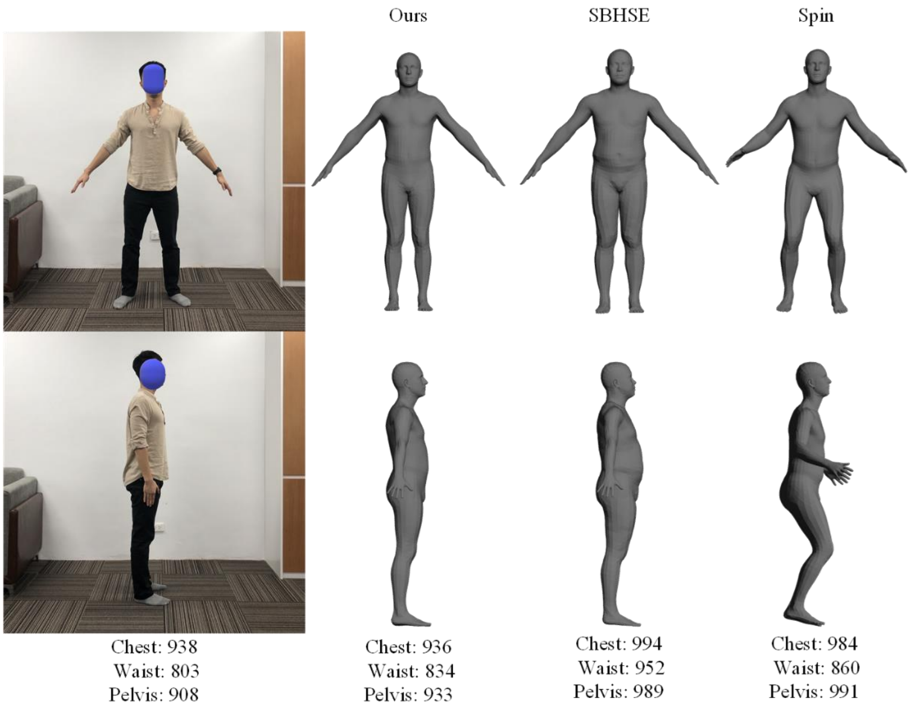

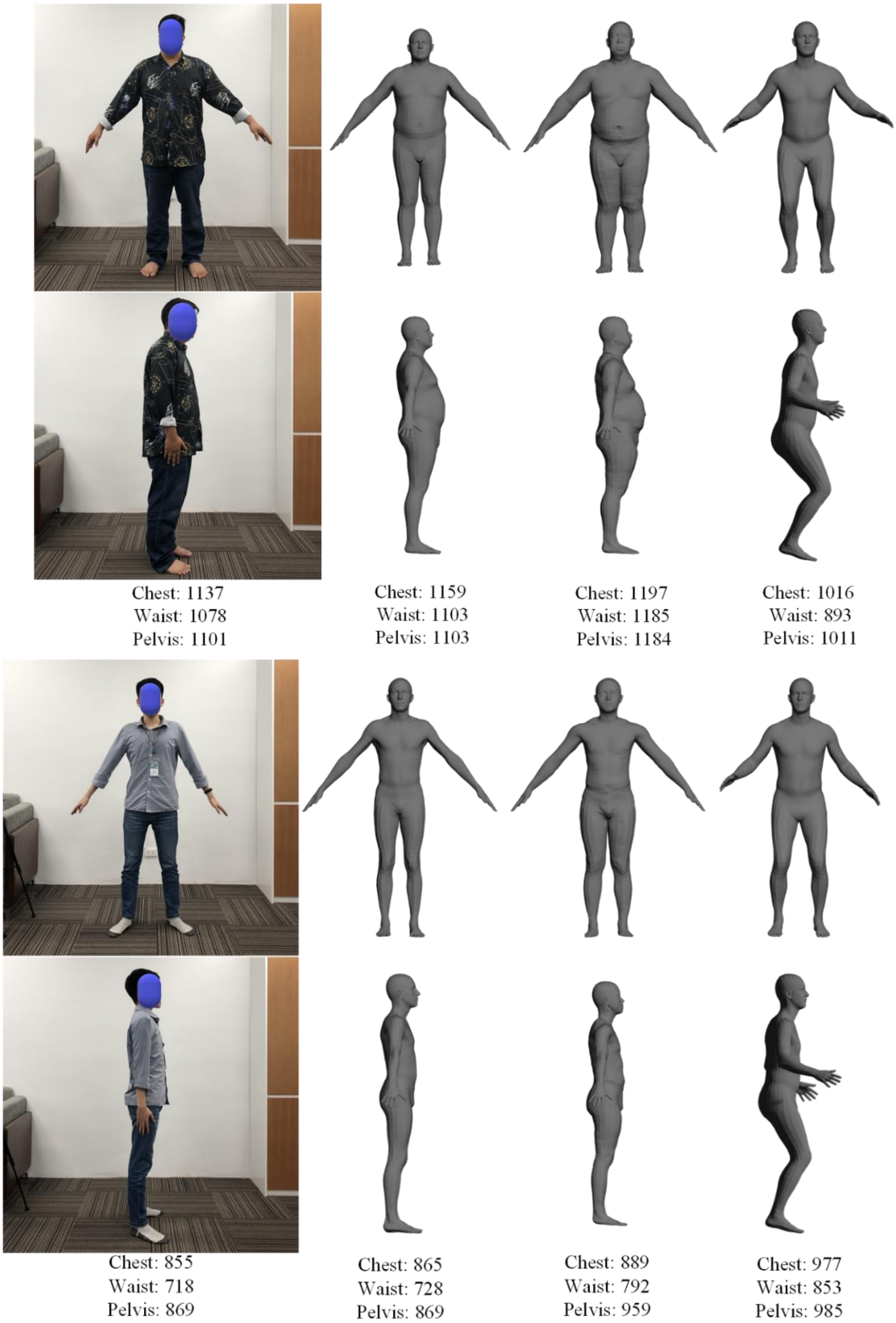

Fig. 6: Qualitative result with different BMI (Underweight, Average, Overweight Obese 1), from left to right: (1) Our method, (2) SBHSE, (3) Spin

5. Conclusion and future work

This research presented a novel approach to reconstruct 3D body human from 2D images and basic measurements such as height and weight. Experiments on the Viettel dataset showed that the proposed method could estimate human body shape and extract anthropometric measurements under clothing with high speed while maintaining accuracy. Together with uncomplicated requirements for device deployment, our method could be applied in various industries, especially in virtual-try on and uniform markets. In the future, more data should be collected to optimize the weight coefficients for different human types to improve the accuracy of the circumference measurements and verify the method on big data.

Appendix A. Mean square errors

Summary of Mean square Error in two genders and two dressing types are summarized in this appendix.

Table A1: Average of mean square error in anthropometric measurements for females without clothes (mm)

No		Detail	Viettel new	SPIN	Silhouettes-based-HSE
1.	1	Head circumference	2.77 ± 2.19	10.09 ± 7.03	9.05 ± 8.18
2.	2	Neck circumference	3.69 ± 2.81	11.31 ± 8.74	4.16 ± 3.00
3.	3	Shoulder to crotch	7.90 ± 4.63	23.26 ± 15.01	3.40 ± 1.79
4.	4	Back length	6.44 ± 3.81	15.31 ± 10.40	2.58 ± 1.73
5.	5	Chest circumference	19.69 ± 15.21	52.74 ± 40.35	11.49 ± 10.60
6.	6	Waist circumference	12.92 ± 10.09	56.56 ± 43.57	15.64 ± 13.03
7.	7	Upper waist circumference	16.98 ± 13.03	55.20 ± 42.12	13.57 ± 12.95
8.	8	Pelvis circumference	16.62 ± 12.81	88.65 ± 52.16	9.78 ± 7.07
9.	9	Wrist circumference	1.48 ± 1.20	7.06 ± 5.11	2.40 ± 1.82
10.	10	Bicep circumference	4.33 ± 3.57	23.24 ± 16.99	10.09 ± 6.93
11.	11	Forearm circumference	1.84 ± 1.61	14.06 ± 9.81	4.66 ± 3.92
12.	12	Arm length	6.93 ± 5.13	42.50 ± 22.27	11.22 ± 9.18
13.	13	Inside leg length	15.11 ± 9.71	81.87 ± 37.96	4.66 ± 2.37
14.	14	Outside leg length	12.96 ± 9.39	89.40 ± 40.81	4.57 ± 3.66
15.	15	Thigh circumference	13.18 ± 9.94	49.25 ± 29.42	7.72 ± 6.71
16.	16	Calf circumference	6.56 ± 5.04	23.56 ± 13.63	5.19 ± 3.87
17.	17	Ankle circumference	3.26 ± 2.39	12.44 ± 7.44	3.77 ± 2.99
18.	18	Height	11.94 ± 10.17	114.71 ± 56.83	0.00 ± 0.00
19.	19	Shoulder breadth	5.00 ± 3.52	9.52 ± 6.53	2.86 ± 2.96
20.	20	Curve shoulder breadth	5.39 ± 3.86	11.12 ± 7.75	27.87 ± 16.88
21.	21	Neck width	1.12 ± 0.86	3.89 ± 2.77	1.65 ± 0.76
22.	22	Bust height	13.26 ± 9.64	98.25 ± 47.25	2.77 ± 1.09
23.	23	Waist height	16.14 ± 10.24	93.70 ± 43.04	4.31 ± 2.02
24.	24	Hip height	14.98 ± 9.90	84.28 ± 39.85	4.60 ± 2.62
25.	25	Back neck height	10.90 ± 9.32	106.40 ± 52.48	2.47 ± 1.66
26.	26	Knee height	9.24 ± 5.98	49.54 ± 23.37	3.45 ± 3.18
27.	27	Inseam	14.09 ± 9.07	76.52 ± 35.45	4.38 ± 3.87
28.	28	Back neck to wrist	6.26 ± 5.26	43.86 ± 24.95	2.27 ± 1.39
29.	29	Back neck to waist	22.62 ± 14.58	60.72 ± 40.72	11.94 ± 9.49
30.	30	Chest width	5.69 ± 4.32	14.89 ± 11.14	4.39 ± 3.57
31.	31	Waist width	3.72 ± 2.81	19.32 ± 14.71	5.40 ± 3.14
32.	32	Pelvis width	6.35 ± 5.15	32.44 ± 18.04	3.51 ± 3.20
33.	33	Finger to finger	10.77 ± 8.56	64.71 ± 37.82	3.85 ± 3.58
34.	34	Wrist to shoulder	3.98 ± 3.19	24.70 ± 13.82	2.15 ± 2.08
35.	35	Wrist to wrist	9.21 ± 7.41	51.59 ± 30.36	3.46 ± 2.76
36.	36	Inseam width	4.20 ± 3.30	19.26 ± 9.60	1.91 ± 2.08

Table A2: Average of mean square error in anthropometric measurements for males without clothes (mm)

No		Detail	Viettel new	SPIN	Silhouettes-based-HSE
1.	1	Head circumference	2.55 ± 1.96	22.84 ± 14.26	8.56 ± 5.21
2.	2	Neck circumference	5.14 ± 3.38	16.15 ± 11.21	6.47 ± 4.38
3.	3	Shoulder to crotch	10.00 ± 5.94	40.87 ± 25.88	3.61 ± 2.27
4.	4	Back length	9.76 ± 4.66	34.74 ± 18.72	2.15 ± 1.45
5.	5	Chest circumference	12.75 ± 9.31	61.11 ± 41.52	12.21 ± 10.75
6.	6	Waist circumference	20.64 ± 14.55	73.91 ± 54.58	16.42 ± 14.01
7.	7	Upper waist circumference	19.92 ± 14.36	65.73 ± 48.19	13.94 ± 11.72
8.	8	Pelvis circumference	16.67 ± 10.67	73.09 ± 47.88	9.00 ± 8.04
9.	9	Wrist circumference	1.76 ± 1.32	12.03 ± 7.82	2.84 ± 1.65
10.	10	Bicep circumference	5.08 ± 3.56	24.97 ± 16.47	6.16 ± 2.07
11.	11	Forearm circumference	2.77 ± 1.73	17.88 ± 11.94	4.00 ± 2.76
12.	12	Arm length	6.13 ± 4.50	34.66 ± 22.40	16.28 ± 12.81
13.	13	Inside leg length	8.77 ± 5.62	49.82 ± 32.83	4.43 ± 2.80
14.	14	Outside leg length	7.57 ± 5.36	55.28 ± 37.39	4.72 ± 2.54
15.	15	Thigh circumference	11.95 ± 8.36	44.15 ± 28.70	10.01 ± 9.12
16.	16	Calf circumference	5.84 ± 4.47	25.49 ± 16.46	5.95 ± 3.97
17.	17	Ankle circumference	4.31 ± 2.60	15.14 ± 9.43	3.28 ± 2.07
18.	18	Height	4.51 ± 3.44	105.35 ± 64.18	0.00 ± 0.00
19.	19	Shoulder breadth	14.55 ± 6.09	17.12 ± 11.25	3.80 ± 2.96
20.	20	Curve shoulder breadth	14.82 ± 6.27	20.02 ± 14.05	32.80 ± 16.01
21.	21	Neck width	3.67 ± 1.52	5.67 ± 3.86	2.07 ± 1.10
22.	22	Bust height	4.77 ± 3.38	72.35 ± 46.88	2.49 ± 1.06
23.	23	Waist height	8.28 ± 5.35	58.25 ± 38.87	3.72 ± 2.61
24.	24	Hip height	8.70 ± 5.68	50.93 ± 34.33	4.61 ± 3.35
25.	25	Back neck height	4.98 ± 3.81	89.68 ± 56.47	2.48 ± 2.42
26.	26	Knee height	5.77 ± 3.68	30.69 ± 20.73	3.92 ± 2.47
27.	27	inseam	8.28 ± 5.36	46.48 ± 30.47	3.85 ± 2.09
28.	28	Back neck to wrist	6.22 ± 5.34	44.79 ± 28.33	1.98 ± 1.68
29.	29	Back neck to waist	34.88 ± 18.70	151.12 ± 82.59	8.86 ± 6.22
30.	30	Chest width	10.04 ± 5.95	20.74 ± 14.05	5.98 ± 5.48
31.	31	Waist width	4.33 ± 2.95	24.76 ± 17.38	5.49 ± 4.86
32.	32	Pelvis width	5.32 ± 3.35	22.55 ± 14.98	4.00 ± 3.15
33.	33	Finger to finger	10.44 ± 9.09	70.85 ± 44.82	5.13 ± 4.79
34.	34	Wrist to shoulder	3.30 ± 2.54	21.58 ± 13.08	2.13 ± 1.90
35.	35	Wrist to wrist	11.56 ± 9.02	53.94 ± 34.90	4.61 ± 3.74
36.	36	Inseam width	2.92 ± 1.90	12.00 ± 7.86	1.62 ± 0.99

Table A3: Average of mean square error in anthropometric measurements for females with clothes (mm)

No		Detail	Viettel new	SPIN	Silhouettes-based-HSE
1.	1	Head circumference	2.83 ± 2.22	11.09 ± 7.52	22.29 ± 15.96
2.	2	Neck circumference	3.73 ± 2.87	13.82 ± 9.25	34.39 ± 22.82
3.	3	Shoulder to crotch	8.14 ± 4.77	20.99 ± 14.38	18.65 ± 12.63
4.	4	Back length	6.71 ± 3.97	13.07 ± 9.29	10.38 ± 7.77
5.	5	Chest circumference	20.28 ± 14.00	71.33 ± 45.37	118.71 ± 76.29
6.	6	Waist circumference	12.94 ± 10.03	79.41 ± 49.41	121.75 ± 86.73
7.	7	Upper waist circumference	17.37 ± 12.46	76.25 ± 48.49	119.85 ± 79.93
8.	8	Pelvis circumference	16.47 ± 12.85	112.77 ± 57.90	105.10 ± 69.58
9.	9	Wrist circumference	1.57 ± 1.19	8.47 ± 5.62	16.55 ± 11.74
10.	10	Bicep circumference	4.40 ± 3.48	32.37 ± 20.03	58.46 ± 31.61
11.	11	Forearm circumference	1.86 ± 1.44	17.66 ± 10.98	37.42 ± 21.43
12.	12	Arm length	6.61 ± 5.19	40.38 ± 22.16	15.12 ± 13.48
13.	13	Inside leg length	14.42 ± 9.79	79.04 ± 38.14	17.80 ± 11.85
14.	14	Outside leg length	12.82 ± 9.37	86.87 ± 41.04	11.90 ± 9.22
15.	15	Thigh circumference	12.84 ± 9.63	63.12 ± 33.47	89.39 ± 59.63
16.	16	Calf circumference	6.56 ± 4.99	27.65 ± 14.81	44.62 ± 30.11
17.	17	Ankle circumference	3.31 ± 2.46	14.46 ± 8.07	23.82 ± 17.84
18.	18	Height	10.80 ± 9.71	107.96 ± 57.17	0.00 ± 0.00
19.	19	Shoulder breadth	5.29 ± 3.96	10.15 ± 6.76	12.54 ± 8.63
20.	20	Curve shoulder breadth	5.50 ± 4.18	12.15 ± 7.85	74.28 ± 50.16
21.	21	Neck width	1.20 ± 0.98	4.50 ± 3.02	8.18 ± 6.06
22.	22	Bust height	12.30 ± 9.70	93.25 ± 47.51	8.41 ± 6.27
23.	23	Waist height	15.25 ± 10.13	91.40 ± 43.08	9.29 ± 7.30
24.	24	Hip height	14.34 ± 9.99	81.73 ± 40.13	15.53 ± 10.87
25.	25	Back neck height	10.02 ± 8.86	100.42 ± 52.75	6.56 ± 4.83
26.	26	Knee height	8.81 ± 6.01	47.72 ± 23.54	12.81 ± 8.65
27.	27	inseam	13.47 ± 9.17	73.92 ± 35.63	18.51 ± 12.12
28.	28	Back neck to wrist	6.59 ± 5.36	41.73 ± 25.28	7.25 ± 5.10
29.	29	Back neck to waist	24.14 ± 15.18	55.58 ± 38.57	59.46 ± 41.22
30.	30	Chest width	5.97 ± 4.88	18.60 ± 12.23	30.05 ± 19.34
31.	31	Waist width	3.79 ± 3.01	26.51 ± 16.44	33.40 ± 25.34
32.	32	Pelvis width	6.43 ± 5.40	40.79 ± 19.55	30.06 ± 20.95
33.	33	Finger to finger	10.87 ± 8.89	62.40 ± 38.49	12.27 ± 11.12
34.	34	Wrist to shoulder	3.94 ± 3.27	21.64 ± 13.32	16.05 ± 10.83
35.	35	Wrist to wrist	9.92 ± 7.73	49.87 ± 31.28	12.62 ± 9.37
36.	36	Inseam width	4.25 ± 3.40	22.88 ± 9.98	15.06 ± 10.61

Table A4: Average of mean square error in anthropometric measurements for males with clothes (mm)

No		Detail	Viettel new	SPIN	Silhouettes-based-HSE
1.	1	Head circumference	2.82 ± 2.16	26.87 ± 16.09	19.34 ± 15.32
2.	2	Neck circumference	5.58 ± 3.49	18.07 ± 13.70	33.87 ± 22.53
3.	3	Shoulder to crotch	9.26 ± 5.65	46.65 ± 26.17	26.19 ± 15.28
4.	4	Back length	8.19 ± 4.75	39.37 ± 18.23	14.68 ± 9.78
5.	5	Chest circumference	13.67 ± 10.01	68.02 ± 49.83	92.31 ± 58.55
6.	6	Waist circumference	20.12 ± 15.37	79.48 ± 58.83	120.04 ± 76.46
7.	7	Upper waist circumference	20.10 ± 14.73	71.15 ± 53.07	105.29 ± 66.43
8.	8	Pelvis circumference	17.24 ± 9.54	79.90 ± 53.24	68.30 ± 49.07
9.	9	Wrist circumference	1.58 ± 1.33	13.87 ± 9.27	21.83 ± 12.37
10.	10	Bicep circumference	5.48 ± 3.79	28.79 ± 20.17	37.49 ± 27.23
11.	11	Forearm circumference	3.11 ± 1.87	20.55 ± 13.85	31.86 ± 18.84
12.	12	Arm length	4.27 ± 3.52	30.14 ± 18.81	24.58 ± 19.45
13.	13	Inside leg length	7.39 ± 5.15	41.01 ± 26.97	20.06 ± 12.68
14.	14	Outside leg length	6.17 ± 3.93	47.00 ± 31.12	15.85 ± 10.83
15.	15	Thigh circumference	12.96 ± 8.98	50.01 ± 32.60	56.65 ± 38.39
16.	16	Calf circumference	6.38 ± 4.40	29.70 ± 19.38	35.33 ± 25.87
17.	17	Ankle circumference	4.50 ± 2.45	17.08 ± 10.77	29.95 ± 17.01
18.	18	Height	4.55 ± 3.61	97.91 ± 57.22	0.00 ± 0.00
19.	19	Shoulder breadth	14.57 ± 6.69	19.18 ± 12.47	13.69 ± 10.08
20.	20	Curve shoulder breadth	14.78 ± 6.94	22.65 ± 15.90	96.78 ± 76.59
21.	21	Neck width	3.62 ± 1.67	6.55 ± 4.70	10.69 ± 7.99
22.	22	Bust height	4.34 ± 3.15	63.76 ± 39.81	6.48 ± 5.04
23.	23	Waist height	6.94 ± 4.96	48.95 ± 32.36	14.58 ± 9.60
24.	24	Hip height	7.07 ± 4.43	42.01 ± 28.18	17.71 ± 11.94
25.	25	Back neck height	5.10 ± 4.09	81.92 ± 49.35	5.70 ± 4.51
26.	26	Knee height	4.35 ± 2.81	25.56 ± 16.91	10.04 ± 7.46
27.	27	inseam	7.11 ± 4.95	38.02 ± 25.09	23.66 ± 13.56
28.	28	Back neck to wrist	7.55 ± 5.81	40.88 ± 24.73	5.00 ± 3.91
29.	29	Back neck to waist	29.92 ± 18.91	170.27 ± 80.58	59.78 ± 38.83
30.	30	Chest width	10.72 ± 6.70	23.70 ± 17.62	31.68 ± 22.16
31.	31	Waist width	4.10 ± 3.15	26.79 ± 19.47	33.06 ± 22.54
32.	32	Pelvis width	5.08 ± 3.02	24.02 ± 16.34	19.47 ± 14.40
33.	33	Finger to finger	12.33 ± 10.04	66.63 ± 40.28	9.63 ± 6.58
34.	34	Wrist to shoulder	2.97 ± 2.48	17.81 ± 11.17	18.90 ± 12.03
35.	35	Wrist to wrist	14.46 ± 9.46	50.78 ± 31.86	9.58 ± 7.00
36.	36	Inseam width	2.98 ± 1.79	12.92 ± 8.29	10.23 ± 7.06

Acknowledgment

The authors would like to thank all members of the 3DR team for their contribution. This research is fully funded by Viettel High Technology Industries Corporation.

Compliance with ethical standards

Conflict of interest

The author(s) declared no potential conflicts of interest with respect to the research, authorship, and/or publication of this article.

References

Bogo F, Kanazawa A, Lassner C, Gehler P, Romero J, and Black MJ (2016). Keep it SMPL: Automatic estimation of 3D human pose and shape from a single image. In the European Conference on Computer Vision, Springer, Amsterdam, Netherlands: 561-578. https://doi.org/10.1007/978-3-319-46454-1_34

Fan J, Yu W, and Hunter L (2004). Clothing Appearance and Fit: Science and technology. Woodhead Publishing, Cambridge, UK. https://doi.org/10.1201/9781439823446

Kanazawa A, Black MJ, Jacobs DW, and Malik J (2018). End-to-end recovery of human shape and pose. In the IEEE conference on computer vision and pattern recognition, Salt Lake City, USA: 7122-7131. https://doi.org/10.1109/CVPR.2018.00744

Liu B, Liu X, Yang Z, and Wang CC (2019). Concise and effective network for 3D human modeling from orthogonal silhouettes. Available online at: https://arxiv.org/abs/1912.11616

Loper M, Mahmood N, Romero J, Pons-Moll G, and Black MJ (2015). SMPL: A skinned multi-person linear model. ACM Transactions on Graphics (TOG), 34(6): 1-16. https://doi.org/10.1145/2816795.2818013

Nguyen DT and Hoang TN (2021). 3D reconstruction human body from anthropometric measurements using diversity control oriented genetic algorithm. MENDEL: Soft Computing Journal, 27: 49-57. https://doi.org/10.13164/mendel.2021.1.049

Pishchulin L, Wuhrer S, Helten T, Theobalt C, and Schiele B (2017). Building statistical shape spaces for 3rd human modeling. Pattern Recognition, 67: 276-286. https://doi.org/10.1016/j.patcog.2017.02.018

Pujades S, Mohler B, Thaler A, Tesch J, Mahmood N, Hesse N, and Black MJ (2019). The virtual caliper: Rapid creation of metrically accurate avatars from 3D measurements. IEEE Transactions on Visualization and Computer Graphics, 25(5): 1887-1897. https://doi.org/10.1109/TVCG.2019.2898748 **PMid:30794512**

Shigeki Y, Okura F, Mitsugami I, and Yagi Y (2018). Estimating 3D human shape under clothing from a single RGB image. IPSJ Transactions on Computer Vision and Applications, 10(1): 1-6. https://doi.org/10.1186/s41074-018-0052-9

Song D, Tong R, Du J, Zhang Y, and Jin Y (2018). Data-driven 3-D human body customization with a mobile device. IEEE Access, 6: 27939-27948. https://doi.org/10.1109/ACCESS.2018.2837147

WHO (2000). Regional office for the Western Pacific: The Asia-Pacific perspective: Redefining obesity and its treatment. World Health Organization, Health Communications Australia, Sydney, Australia.

Wuhrer S and Shu C (2013). Estimating 3D human shapes from measurements. Machine Vision and Applications, 24(6): 1133-1147. https://doi.org/10.1007/s00138-012-0472-y

Zeng Y, Fu J, and Chao H (2017). 3D human body reshaping with anthropometric modeling. In the International Conference on Internet Multimedia Computing and Service, Springer, Qingdao, China: 96-107. https://doi.org/10.1007/978-981-10-8530-7_10

Zhang C and Chen T (2001). Efficient feature extraction for 2D/3D objects in mesh representation. In the International Conference on Image Processing (Cat. No. 01CH37205), IEEE, Thessaloniki, Greece, 3: 935-938. https://doi.org/10.1109/ICIP.2001.958278